Coherent adiabatic transport of atoms in radio-frequency traps

T. Morgan, B. O'Sullivan, and Th. Busch
Department of Physics, University College Cork, Cork, Ireland
(Received 21 March 2011; published 19 May 2011)

Coherent transport by adiabatic passage has recently been suggested as a high-fidelity technique to engineer the center-of-mass state of single atoms in inhomogeneous environments. While the basic theory behind this process is well understood, several conceptual challenges for its experimental observation have still to be addressed. One of these is the difficulty that currently available optical or magnetic micro-trap systems have in adjusting the tunneling rate time dependently while keeping resonance between the asymptotic trapping states at all times. Here we suggest that both requirements can be fulfilled to a very high degree in an experimentally realistic setup based on radio-frequency traps on atom chips. We show that operations with close to 100% fidelity can be achieved and that these systems also allow significant improvements for performing adiabatic passage with interacting atomic clouds.

DOI: 10.1103/PhysRevA.83.053620 PACS number(s): 03.75.−b, 05.60.Gg, 67.85.−d

I. INTRODUCTION

Going beyond nanotechnologies and engineering quantum systems on the basis of single particles has in recent years been one of the most exciting and active areas of physics [1]. Due to the fragile nature of single-particle quantum states, quantum engineering techniques need to be fault tolerant and lead to high fidelities on every application to avoid the large and costly overhead that comes with error-correction schemes [2]. Comprising one class of techniques that can achieve this are so-called adiabatic techniques and their use in optical systems has been widely investigated in the past. In particular, stimulated Raman adiabatic passage (STIRAP) is one adiabatic technique that allows the transfer of the populations from one electronic state to another with 100% fidelity [3]. It relies on the existence of a so-called dark state in a three-level system and requires a counterintuitive pulse sequence to coherently couple the individual levels.

Recently, it has been shown that similar techniques can, in principle, be used to control the quantized center-of-mass state of single particles [4–6]. This atom-optical analog has been dubbed coherent transport by adiabatic passage (CTAP) and while the possibility of observing this process has received significant attention [7,8], the conditions that have to be fulfilled for its observation are currently hard to achieve experimentally. In particular, all states involved are required to be in resonance during the whole process. However, since the strength of the tunnel coupling is usually adjusted by changing the distance between the microtraps, which leads to significant overlap of the neighboring trapping potentials, the eigenstates become time dependent. Several solutions to the problem have been suggested, all involving significant experimental resources or restrictions on the parameter space [4,6,7]. A similar process coupling classical light between optical waveguides has recently been experimentally demonstrated [9–11].

Here we propose a simple experimental setup that fulfills all necessary conditions to observe CTAP for cold atoms. Our proposal is based on radio-frequency (rf) traps, which have recently become one of the most versatile tools for trapping cold atoms [12,13]. The advantage of rf systems is that their physics is well known, they are relatively benign systems to work with experimentally, and they are widely available today. They not only allow us to create standard trapping potentials [12] but can also be used to coherently manipulate matter waves [13,14] or create complicated, nonstandard trapping geometries [15–17].

We will also show that our setup offers the possibility for extending adiabatic techniques to clouds of interacting atoms. The presence of interaction between the atoms introduces nonlinearities into the system [18] which have been shown to inhibit the effectiveness of CTAP in transporting atoms [7]. Several strategies to adjust the process and to allow transport in the presence of these nonlinear interactions have been suggested, for example a fixed detuning between the potential wells [19]. Here we will show that dynamically controlling the detuning between the potentials provides a marked improvement in the state transfer efficiency over both regular and fixed detuning CTAP.

In the following we will first briefly review the idea of CTAP for ultracold atoms. In Sec. III we will outline the theoretical description of rf trapping and describe the system needed for CTAP. In Sec. IV we demonstrate atomic transport in this system and show that the process allows high-fidelity atomic transport in contrast to the intuitive method, which fails. In Sec. V we examine the transport of an interacting atomic cloud and how the presence of nonlinear interaction can be compensated for by dynamic detuning. Finally, in Sec. VI we conclude.

II. COHERENT TRANSPORT ADIABATIC PASSAGE

To briefly review the process of adiabatic population transfer let us consider a system of three ground states in three identical microtraps, $|0\rangle_L$,$|0\rangle_M$, and $|0\rangle_R$ (see Fig. 1). In a linear arrangement the only tunnel couplings that are significant are J_{LM} for the transition $|0\rangle_L \rightarrow |0\rangle_M$ and J_{MR} for $|0\rangle_M \rightarrow |0\rangle_R$. By assuming that the three states are in resonance when isolated, the Hamiltonian for such a system is given by

$$H(t) = \hbar \begin{pmatrix} 0 & -J_{LM}(t) & 0 \\ -J_{LM}(t) & 0 & -J_{MR}(t) \\ 0 & -J_{MR}(t) & 0 \end{pmatrix} . \qquad (1)$$

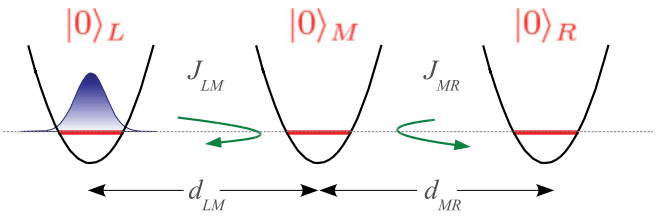

FIG. 1. (Color online) Schematic of the CTAP process for an atom in the left trap. Reducing the distances between the traps leads to an increase in the tunneling strengths.

and a smooth time dependence of the tunneling coupling pulses can be achieved by continuously changing the distances between the traps, $d_{LM}(t)$ and $d_{MR}(t)$. The eigenstates of this Hamiltonian are very well known [3] and of particular interest to our work here is the so-called dark state

$$|d\rangle = \cos\theta|0\rangle_L - \sin\theta|0\rangle_R \tag{2}$$

for which the mixing angle θ is given by

$$\tan\theta = J_{LM}/J_{MR}. \tag{3}$$

This state has a nondegenerate zero eigenvalue and therefore an adiabatic evolution will guarantee that the system, once prepared in $|d\rangle$, will always stay in it. Note that, as the only contribution to $|d\rangle$ from the state $|0\rangle_M$ comes through the mixing angle, the system has zero probability of being found in $|0\rangle_M$ at any time.

The CTAP process can now be understood by considering an atom initially in the state $|0\rangle_L$. Increasing and decreasing J_{MR} before J_{LM}, which is counterintuitive to traditional tunneling schemes, continuously decreases the population in state $|0\rangle_L$ and increases the population in state $|0\rangle_R$, leading to a 100% transfer at the end of the process.

It is worth stressing again the conditions that have to be fulfilled for the above dynamics to occur. First, the process must be adiabatic with respect to the energy level splitting in the harmonic oscillators, which means that the movement of the traps has to be slow and the whole process must take longer than $\omega_{\rm HO}^{-1}$, where $\omega_{\rm HO}$ is the harmonic oscillator frequency of the individual traps. As typical numbers of $\omega_{\rm HO}$ for microtraps are in the kilohertz regime, this means that the time required for this process is much shorter than lifetimes of the trapped atoms, which makes this process a promising tool for quantum information. The other condition we require, as previously mentioned, is that all single trap states are in resonance at any point in time, which is difficult to achieve once the trapping potentials start to overlap.

In the next section we will demonstrate how the second condition can be fulfilled in an experimentally realistic system using radio-frequency potentials.

III. RADIO-FREQUENCY TRAPPING

Radio-frequency trapping relies on the process of coupling magnetic sublevels in the presence of an inhomogeneous magnetic field [12–15]. Consider a hyperfine atomic ground state with total spin $F = \frac{1}{2}$. In the presence of a magnetic field the two hyperfine sublevels $m_F = \frac{1}{2}$ and $m'_F = -\frac{1}{2}$ are split by an amount $\mu_B g_F m_F B$, where g_F is the atomic g factor of the hyperfine level and μ_B is the Bohr magneton. Irradiating such a system with a linearly polarized radio frequency, $\mathbf{B}_{\rm rf}\cos(\omega t)$, couples the sublevels $|\frac{1}{2},\frac{1}{2}\rangle \leftrightarrow |\frac{1}{2},-\frac{1}{2}\rangle$ with spatial resolution due to the spatial dependence of the magnetic field. Here we will concentrate on a one-dimensional (1D) description of such a process, which is valid when the radio frequency and magnetic field are orthogonal to each other. By assuming the inhomogeneous magnetic field to be oriented in the x direction, $B = B(x)$, the Hamiltonian of the coupled system can be written as

$$H(x) = \frac{1}{2}\begin{pmatrix} \mu_B g_F B(x) - \hbar\omega & \hbar\Omega \\ \hbar\Omega & -\mu_B g_F B(x) + \hbar\omega \end{pmatrix}, \tag{4}$$

where the strength of the coupling is given by the Rabi frequency [20]

$$\Omega = \frac{\mu_B g_F}{4\hbar}|\mathbf{B}_{\rm rf}\times\hat{e}_B|\sqrt{F(F+1) - m_F m'_F}\,, \tag{5}$$

and where $\hat{e}_B$ is the orientation of the local static magnetic field. The eigenvalues of this Hamiltonian are [15]

$$E_\pm(x) = \pm\frac{1}{2}\sqrt{\hbar^2\Omega^2 + [\mu_B g_F B(x) - \hbar\omega]^2}, \tag{6}$$

$$\approx \pm\frac{1}{2}[\mu_B g_F B(x) - \hbar\omega] \pm \frac{\hbar^2\Omega^2}{4[\mu_B g_F B(x) - \hbar\omega]}, \tag{7}$$

where the second expression is valid far from resonance, $\hbar\Omega \ll [\mu_B g_f B(x) - \hbar\omega]$. The second term in the expression can be viewed as a Stark shift on the energy levels.

To create a multiwell potential it is necessary to use several frequencies and the above analysis will become significantly more complicated. However, if we assume that the individual frequencies are spaced sufficiently far apart and have low Rabi frequencies with respect to the detuning, we can approximate the dynamics locally by considering only the nearest resonance frequency, $\omega(x) = \omega_{n(x)}$ [15]. Formally, this means that n is chosen such that $[\mu_B g_F B(x) - \hbar\omega_{n(x)}]$ is minimized at any position x. The effects of the combined Stark shifts, produced by the frequencies not closest to resonance, can then be summed as [15]

$$L_n(x) = \sum_{j\neq n}\frac{\hbar^2\Omega^2}{4[\mu_B g_F B(x) - \hbar\omega_{j(x)}]}, \tag{8}$$

so that the eigenvalues are given by

$$E_\pm(x) = \pm\tfrac{1}{2}\sqrt{\hbar^2\Omega^2 + [\mu_B g_F B(x) - \hbar\omega + 2L_n(x)]^2}. \tag{9}$$

From this, and by considering that the couplings are strong enough to yield a Landau-Zener transition probability close to unity, the resulting adiabatic potential is given by

$$V_{ad,\pm}(x) = (-1)^{n(x)}\left[E_\pm(x) \mp \frac{\hbar\omega_{n(x)}}{2}\right] \mp \sum_{k=1}^{n(x)-1}(-1)^k\hbar\omega_k. \tag{10}$$

To produce a radio-frequency potential with three minima along the x direction we will need six different radio frequencies. In the following we will assume that the 1D linear magnetic field is given by $B(x) = bx$, where b is the magnetic field gradient. For convenience we choose five of the six radio frequencies to be equally spaced initially,

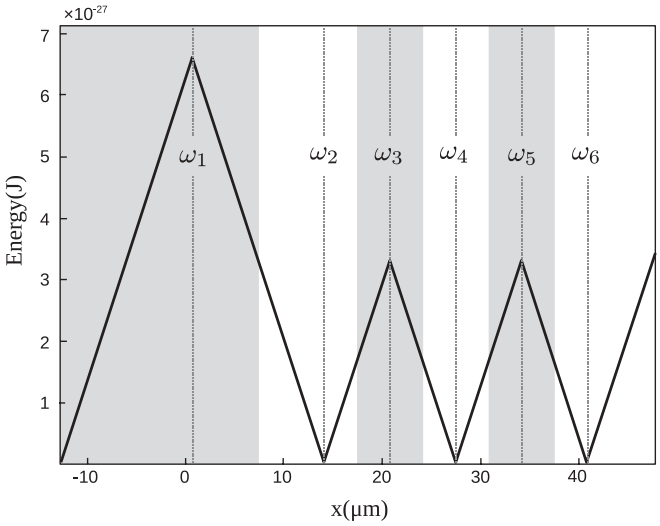

FIG. 2. Trapping potential created by six radio frequencies $\omega_1 = 2\pi \times 1000$ kHz and $\omega_n = 2\pi n \times 10\,000$ kHz, $n = 2 : 6$. Their resonance positions are marked by the broken vertical lines and the range over which they are applied is indicated by the gray and white zones. The magnetic field gradient has strength $b = 160$ G cm^{-1} and $g_F = -\frac{2}{3}$ for the ^{87}Rb ground state $^2S_{\frac{1}{2}}$. The Rabi frequency is chosen to be $2\pi \times 50$ kHz. The traps resemble harmonic oscillator potentials close to each minima.

$\omega_n = 2n\pi \times 10\,000$ kHz ($n = 2 : 6$), which produces three equidistant minima. The first radio frequency ω_1 does need to have the same distance as the other frequencies, as its value only controls the height of the first maximum (see Fig. 2) and can therefore be adjusted without changing the trap geometry in the area where tunneling takes place. For our potential we set $\omega_1 = 2\pi \times 1000$ kHz and in Fig. 2 we indicate the local frequencies and show the resulting adiabatic potential in the positive x direction.

IV. ADIABATIC PASSAGE

In this section we will apply the CTAP procedure to a single atom trapped in a three-well rf potential. We will show that the strong decay of the influence of the radio frequencies away from their respective resonance points allows us to fulfill the resonance condition between the asymptotic eigenstates at all times during the process. While the Stark shift from neighboring resonances cannot be neglected, it is small enough to not destroy the process.

Movement of the traps is achieved by changing the individual radio frequencies that are associated with each trap. Traditionally for CTAP the middle trap is chosen to be at rest and the two outer ones are moving inward and outward (see also Fig. 1). Here we will choose a slightly different, but of course completely analogous, route in that we keep the position of the left trap fixed. This allows us to keep the values of the minima equal, which is essential to satisfy the condition of resonance between all traps.

In order to achieve CTAP when moving the traps in this nontraditional manner the approach of the right trap toward the middle must start earlier than the approach of the middle trap to the left. One therefore initially only changes the frequencies ω_5 and ω_6, which determine the shape and position of the right-hand-side trap. After a delay τ, the two frequencies ω_3 and ω_4 are changed as well, allowing the middle trap to move toward the left. Due to the adiabatic nature of the process the exact shape of this time-dependent frequency adjustment, $f(t)$, does not matter and we can formalize this process as

$$\omega_1(t) = \omega_1(t_0), \tag{11a}$$
$$\omega_2(t) = \omega_2(t_0), \tag{11b}$$
$$\omega_3(t) = \omega_3(t_0) - \tfrac{1}{2} f(t-\tau)\theta(t-\tau), \tag{11c}$$
$$\omega_4(t) = \omega_4(t_0) - f(t-\tau)\theta(t-\tau), \tag{11d}$$
$$\omega_5(t) = \omega_5(t_0) - \tfrac{1}{2} f(t) - f(t-\tau)\theta(t-\tau), \tag{11e}$$
$$\omega_6(t) = \omega_6(t_0) - f(t) - f(t-\tau)\theta(t-\tau), \tag{11f}$$

where $\theta(t)$ is the Heaviside step function. In Fig. 3(a) these changes are shown for the typical system considered here and the resulting movements of the trap minima are displayed in Fig. 3(b). As can been seen, the minimum of the left trap remains stationary while the other traps are moving toward and away from it. The resulting movement between neighboring traps exactly fulfills the requirement of the CTAP process, leading to the desired increase and decrease in the tunneling strength between initially the middle and right traps before the increase and decrease in tunneling strength between the left and middle traps.

To demonstrate adiabatic passage for single atoms and for typical experimentally realistic parameters, we will in the following show the results of numerical simulations of the full Schrödinger equation. We choose a single ^{87}Rb atom to be initially located in the center-of-mass ground state of the left trap and start the process described in Sec. IV with an initial separation between the radio frequencies of $2\pi \times 10\,000$ kHz. The minimum distance to which the frequencies approach each other is $2\pi \times 200$ kHz, which ensures that we are always in the regime of tunneling interaction, as the minimum barrier height

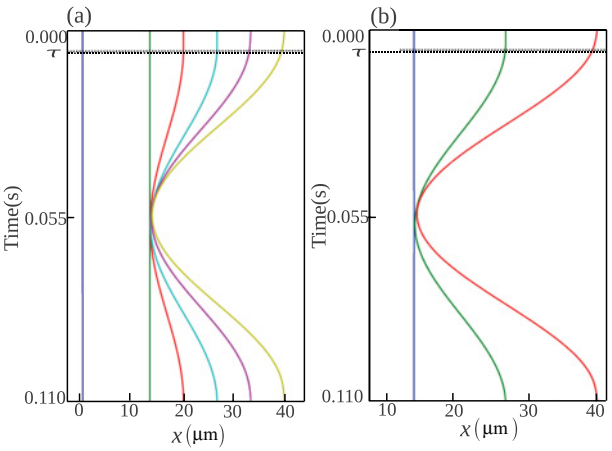

FIG. 3. (Color online) (a) Radio frequencies, ω_n, as a function of time to achieve the counterintuitive positioning sequence. (b) Positions of the trap minima as a function of time. The left trap remains stationary while the other two traps move toward it. The delay in the movement of the middle trap in comparison to the right trap ($\tau = 0.0055$ s) is indicated by the broken line.

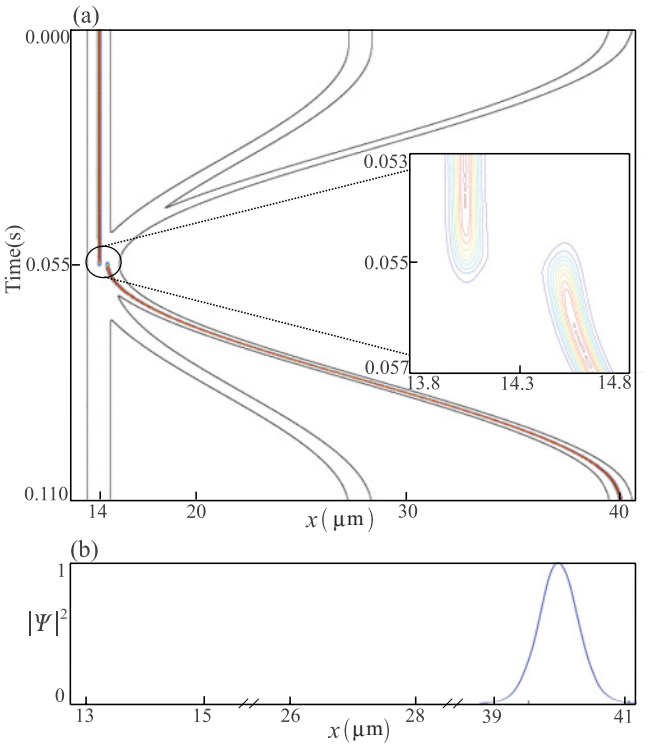

FIG. 4. (Color online) (a) Probability density for a single atom initially located in the trap on the left-hand side with respect to time for counterintuitive trap movement. The inset shows the tunneling area in greater detail. (b) Density of the final state in each of the three traps.

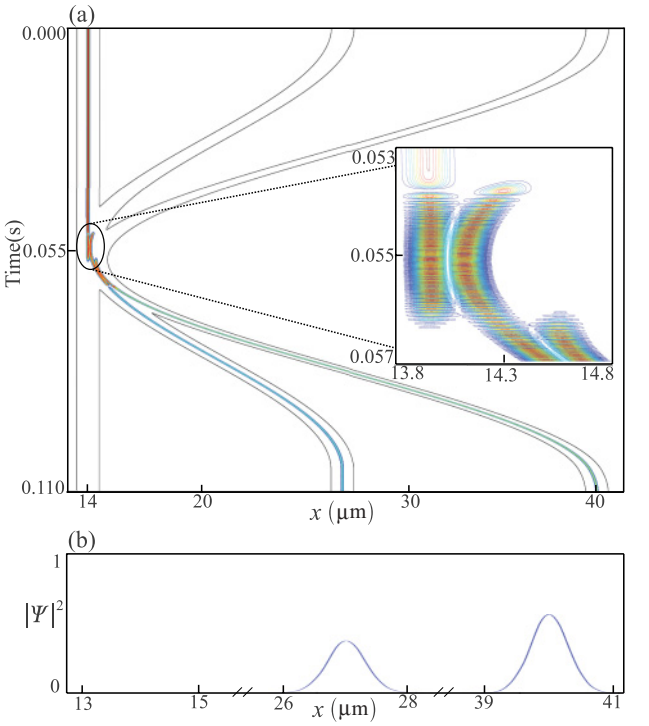

FIG. 5. (Color online) (a) Probability density for a single atom initially located in the trap on the left-hand side with respect to time for intuitive trap movement. The inset shows the tunneling area in greater detail, where Rabi oscillations between neighboring traps are clearly visible. (b) Density of the final state in each of the three traps.

between the individual traps is 5.3313×10^{-29} J at the point of closest approach, compared to the ground-state energy of 1.3615×10^{-29} J. The form of the adjustment function $f(t)$ is taken to be a cosine and for numerical simplicity we restrict ourselves to one spatial dimension.

In Fig. 4 we show the probability density function with respect to time for the CTAP process. The overall time for this process is chosen to be $T = 0.11$ s, which is large compared to the approximate harmonic oscillator frequency of the individual traps of $\omega_{\mathrm{HO}}^{-1} \approx 4 \times 10^{-6}$ s, and we are therefore assured that the system is at all times in the dark eigenstate. This can also be seen from the fact that the probability for being in the middle trap at any time is zero. The process leads to high-fidelity population transfer and an absence of Rabi oscillations.

To compare the above situation to a process in which direct tunneling between two neighboring traps plays an important role, we show in Fig. 5 the results of the same process, this time however using an intuitive trap movement. The direct tunneling is clearly manifest in the appearance of Rabi oscillations between the traps and the process therefore does not deliver the required robust population transfer. In fact, the final state becomes highly susceptible to variations of the system parameters [21].

We have confirmed that these results are representative for a large range of parameters, making rf traps ideal systems to investigate general adiabatic processes.

V. NONLINEAR SYSTEMS

The extension of adiabatic methods to nonlinear systems is of great importance not only to describe experimental situations but also for the understanding of the underlying physical principles [18,19,22,23]. In this section we show how CTAP can be used with time-dependent potentials to coherently transport a cloud of interacting, Bose-condensed atoms. For this, we treat the adiabatic process as a series of stationary states which can be described by the time-independent Gross-Pitaevskii equation

$$\mu\Psi(x) = \left(-\frac{\hbar^2}{2m}\nabla^2 + V(x) + g_{1D}|\Psi|^2\right)\Psi(x), \qquad (12)$$

where $V(x)$ is the external potential and μ is the chemical potential at each respective point in time. The one-dimensional interaction strength between bosons with a three-dimensional s-wave scattering length a_s is given by $g_{1D} = \frac{4N\hbar^2 a_s}{m a_\perp}(a_\perp - Ca_s)^{-1}$ [24]. The trap width in the radial direction is given by $a_\perp$ and $C \approx 1.4603$. In the three-level approximation the Hamiltonian can therefore be written as

$$H(t) = \hbar \begin{pmatrix} \hbar\omega_L + \mu_L & -J_{LM}(t) & 0 \\ -J_{LM}(t) & \hbar\omega_M & -J_{MR}(t) \\ 0 & -J_{MR}(t) & \hbar\omega_R + \mu_R \end{pmatrix}, \qquad (13)$$

where μ_L and μ_R are the chemical potentials associated with the atomic clouds in the left or right trap, respectively, and ω_L, ω_M, and ω_R are the harmonic oscillator frequencies associated

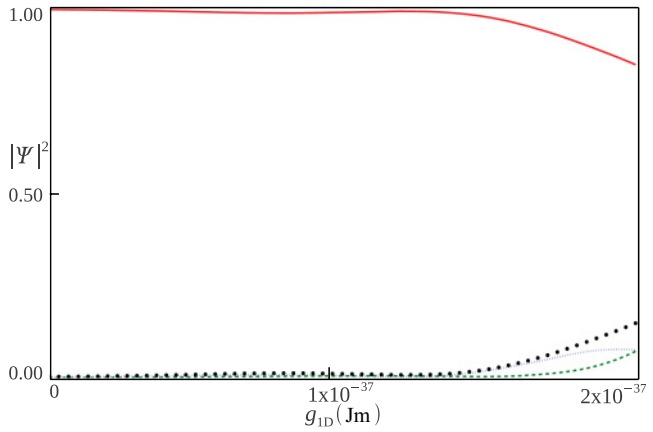

FIG. 6. (Color online) Final population in left (vertical dashed line, blue), middle (horizontal dashed line, green), and right (solid line, red) traps with increasing interaction strength. The dotted black line shows the total population not occupying the target (right) trap. The maximum value of g_{1D} corresponds to $\mu = 1.4318 \times 10^{-29}$ J, which is smaller than $\hbar\omega_{L,M,R}$ at all times.

with the individual traps. Note that this Hamiltonian has been extensively investigated for constant couplings between the traps [25,26]. As the particle number in each individual trap is a function of time, the chemical potentials μ_i will change and destroy the resonances between the traps. To compensate for this we will in the following allow for the trapping frequencies to be functions of time as well. Starting with a cloud of atoms in the left trap, it is clear that the chemical potential μ_L will decrease durning the process, while μ_R will increase. Adjusting the trapping frequencies ω_L and ω_R can restore the resonance between the uncoupled traps by ensuring that $\hbar\omega_i + \mu_i \approx$ constant at all times. However, in order to be able to make the three-state approximation, we need to make sure that $\mu_i < \hbar\omega_i$ for all values of μ_i and ω_i. This means in practice that the process is limited to cold atomic clouds with small nonlinearities.

Using the same radio-frequency potential as in the linear case, we place a cloud of interacting ^{87}Rb atoms in the ground state of the left trap by determining the solution to the Gross-Pitaevskii equation for an isolated trapping potential. To show the influence of the nonlinear behavior, we first carry out the same counterintuitive trap movements as in the linear section without time-dependent change in the trapping frequencies. In Fig. 6 we show the final populations in the individual traps as a function of increasing values for g_{1D}. It is immediately obvious that even for weak interactions the nonlinear term is disruptive to the process of CTAP. In fact, for $g_{1D} = 2 \times 10^{-37}$ J m the state transfer efficiency is reduced to 84%. By choosing a typical radial trap width of 130 nm, this value of g_{1D} corresponds to $N = 2$ for ^{87}Rb.

As outlined above, to restore resonance in the presence of a changing chemical potential we must adjust the trapping frequency so that at any point in time $\hbar\omega_L(t) + \mu_L(t) = \hbar\omega_M = \hbar\omega_R(t) + \mu_R(t)$. However, determining the required adjustments is not a simple exercise for at least two reasons. First, the density dependence of the chemical potential will prevent this change from simply being linear in time, and, second, a conceptual difficulty in determining the individual chemical potentials arises when the traps are close together. While one could try to calculate the chemical potential, and therefore the on-site energies, in all traps at all times to a good approximation, this is certainly not experimentally possible. In the following, we therefore suggest a simple functional form for dynamically detuning the outer traps and we show that it allows us to achieve significantly higher transfer than possible without adjustments. A similar idea, however without time dependence, was recently proposed by Graefe *et al.* [19], who showed that by detuning the left and the right traps by the same fixed amount throughout the process an improved transfer of population can be achieved.

The outline of our scheme for dynamic detuning is as follows. Initially the cloud is trapped in the left trap, which we detune such that resonance with the eigenstates of the other two traps is ensured (since the traps are far apart, it is possible to determine the chemical potential μ_L). As we time evolve the system, tunneling sets in and we begin to reduce the detuning on the left trap to zero while increasing the detuning of the right trap, as atoms enter it. This can be achieved by adjusting the radio frequencies ω_2 and ω_6, associated with the left- and right-hand-side traps, respectively. Here we suggest that a good form of function for the adjustment related to the left-hand-side trap is

$$\Delta\omega_2(\kappa;\tilde{t}) = \tfrac{1}{2}[1 - \tanh(\kappa\tilde{t})]\Delta\omega_0, \tag{14}$$

where the initial value for the change in ω_2 is given by ω_0. The function runs between $\Delta\omega_0$ and 0 and the steepness in the crossover region is determined by κ. This gives us an effective handle on both the time when the adjustment starts and the duration of the adjustment (see inset of Fig. 7). Here $\tilde{t} = t - T/2$, with T being the overall duration of the process. At the same time the frequency of the right-hand-side trap

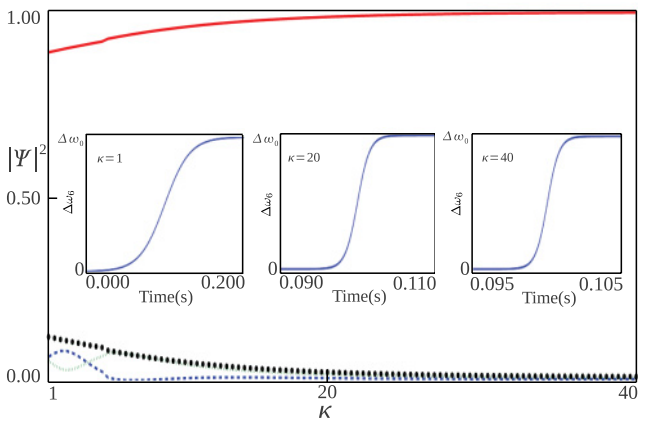

FIG. 7. (Color online) Final population in left (horizontal dashed blue line), middle (vertical dashed green line), and right (solid red line) traps for nonlinear CTAP with increasing κ and $\Delta\omega_0 = 2\pi \times 1.5$ kHz. The dotted black line shows the total population not occupying the target (right) trap. The insets show the shape of $\Delta\omega_6(\kappa;\tilde{t})$ for different values of κ. An increased value of κ increases the time when the adjustment begins and decreases the adjustment time.

needs to be adjusted as well and it is easy to see that a mirror-symmetric change in ω_6 is the best choice:

$$\Delta\omega_6(\kappa;\tilde{t}) = \tfrac{1}{2}[1+\tanh(\kappa\tilde{t})]\Delta\omega_0, \tag{15}$$

The dynamic adjustments of the radio-frequency equations (IV) then become

$$\omega_1(t) = \omega_1(t_0), \tag{16a}$$
$$\omega_2(t) = \omega_2(t_0) - \Delta\omega_2(\kappa,\tilde{t}), \tag{16b}$$
$$\omega_3(t) = \omega_3(t_0) - \tfrac{1}{2}f(t-\tau)\theta(t-\tau), \tag{16c}$$
$$\omega_4(t) = \omega_4(t_0) - f(t-\tau)\theta(t-\tau), \tag{16d}$$
$$\omega_5(t) = \omega_5(t_0) - \tfrac{1}{2}f(t) - f(t-\tau)\theta(t-\tau), \tag{16e}$$
$$\omega_6(t) = \omega_6(t_0) - f(t) - f(t-\tau)\theta(t-\tau) + \Delta\omega_6(\kappa,\tilde{t}). \tag{16f}$$

In Fig. 7 we show the final population transferred to the right trap for increasing values of κ and for $\Delta\omega_0 = 2\pi \times 1.5$ kHz. We can see that the dynamic adjustment of the detunings of the outer traps allows us to achieve population transfer of $>99\%$, up from 84%. This is an improvement over both standard CTAP and fixed detuning in the weak-interaction regime and, in fact, returns to the transfer efficiency of single-particle CTAP.

VI. CONCLUSIONS

We have shown that radio-frequency traps can be used as microtraps for processes in which an adjustable tunneling strength is required. Neighboring trapping potentials can be overlapped without significantly changing the underlying energy level structure. This property has allowed us to create a triple-well radio-frequency potential in which coherent transport using adiabatic passage can be demonstrated. For a single atom, it was shown that complete transfer between the left and right traps by utilizing the dark state of the system is possible, maintaining the advantages of an absence of Rabi oscillations and robustness against variation in system parameters.

For a cloud of weakly interacting atoms we have demonstrated a technique that significantly improves the efficiency of CTAP by dynamically detuning the outer traps. Our suggested setup is close to experimental realities, avoids the large overhead of other suggestions, and can easily be extended to other adiabatic techniques.

ACKNOWLEDGMENTS

The authors would like to thank Peter Krüger and Thomas Fernholz for valuable discussions. This work was supported by Science Foundation Ireland under Projects No. 05/IN/I852 and No. 10/IN.1/I2979. BOS acknowledges support from IRCSET through the Embark Initiative No. RS/2006/172.

[1] M. A. Nielsen and I. L. Chuang, *Quantum Computation and Quantum Information* (Cambridge University Press, Cambridge, 2000).
[2] A. M. Steane, Phys. Rev. Lett. **77**, 793 (1996).
[3] K. Bergmann, H. Theuer, and B. W. Shore, Rev. Mod. Phys. **70**, 1003 (1998).
[4] K. Eckert, M. Lewenstein, R. Corbalán, G. Birkl, W. Ertmer, and J. Mompart, Phys. Rev. A **70**, 023606 (2004).
[5] A. D. Greentree, J. H. Cole, A. R. Hamilton, and L. C. L. Hollenberg, Phys. Rev. B **70**, 235317 (2004).
[6] K. Eckert, J. Mompart, R. Corbalán, M. Lewenstein, and G. Birkl, Opt. Commun. **264**, 264 (2006).
[7] M. Rab, J. H. Cole, N. G. Parker, A. D. Greentree, L. C. L. Hollenberg, and A. M. Martin, Phys. Rev. A **77**, 061602 (2008).
[8] B. O'Sullivan, P. Morrissey, T. Morgan, and Th. Busch, Phys. Scr. T **140**, 014029 (2010).
[9] S. Longhi, Phys. Rev. E **73**, 026607 (2006).
[10] S. Longhi, G. Della Valle, M. Ornigotti, and P. Laporta, Phys. Rev. B **76**, 201101(R) (2007).
[11] A. A. Rangelov, N. V. Vitanov, and B. W. Shore, J. Phys. B **42**, 055504 (2009).
[12] O. Zobay and B. M. Garraway, Phys. Rev. Lett. **86**, 1195 (2001).
[13] T. Schumm, S. Hofferberth, L. M. Andersson, S. Wildermuth, S. Groth, I. Bar-Joseph, J. Schmiedmayer, and P. Krüger, Nature Phys. **1**, 57 (2005).
[14] S. Hofferberth, B. Fischer, T. Schumm, J. Schmiedmayer, and I. Lesanovsky, Phys. Rev. A **76**, 013401 (2007).
[15] Ph. W. Courteille, B. Deh, J. Fortágh, A. Günther, S. Kraft, C. Marzok, S. Slama, and C. Zimmermann, J. Phys. B **39**, 1055 (2006).
[16] I. Lesanovsky, T. Schumm, S. Hofferberth, L. M. Andersson, P. Krüger, and J. Schmiedmayer, Phys. Rev. A **73**, 033619 (2006).
[17] T. Fernholz, R. Gerritsma, P. Krüger, and R. J. C. Spreeuw, Phys. Rev. A **75**, 063406 (2007).
[18] J. Liu, B. Wu, and Q. Niu, Phys. Rev. Lett. **90**, 170404 (2003).
[19] E. M. Graefe, H. J. Korsch, and D. Witthaut, Phys. Rev. A. **73**, 013617 (2006).
[20] W. Ketterle and N. J. van Druten, Adv. Mol. Opt. Phys. **37**, 181 (1996).
[21] J. Mompart, K. Eckert, W. Ertmer, G. Birkl, and M. Lewenstein, Phys. Rev. Lett. **90**, 147901 (2003).
[22] A. Smerzi, S. Fantoni, S. Giovanazzi, and S. R. Shenoy, Phys. Rev. Lett. **79**, 4950 (1997).
[23] I. Marino, S. Raghavan, S. Fantoni, S. R. Shenoy, and A. Smerzi, Phys. Rev. A **60**, 487 (1999).
[24] M. Olshanii, Phys. Rev. Lett. **81**, 938 (1998).
[25] G.-F. Wang, D.-F. Ye, L.-B. Fu, X.-Z. Chen, and J. Liu, Phys. Rev. A **74**, 033414 (2006).
[26] B. Liu, L.-B. Fu, S.-P. Yang, and J. Liu, Phys. Rev. A **75**, 033601 (2007).